Characterisation of local homogenized complex young's modules of curved beam in composite material by using an inverse method and a finite element operator

Paul Bottois, Frédéric Ablitzer, Nicolas Joly, Charles Pezerat

NOVEM 2018
Noise and vibration emerging methods
The 6th conference, 7 – 9 May 2018
Ibiza – Spain

CHARACTERISATION OF LOCAL HOMOGENIZED COMPLEX YOUNG'S MODULES OF CURVED BEAM IN COMPOSITE MATERIAL BY USING AN INVERSE METHOD AND A FINITE ELEMENT OPERATOR

P. BOTTOIS*, F. ABLITZER, N.J OLY and C. PÉZERAT

Laboratoire d'Acoustique de l'Université du Mans (LAUM), FRANCE

ABSTRACT

Identification of elastic and damping properties is a challenge for fabrication of composite materials, which can have complex shapes. A new approach based on the Force Analysis Technique (FAT) was developed to identify structural parameters from local equation of motion. For structures with known analytical models, this method worked well. This work presents a similar approach to extend the previous method to the structure which can be described with known analytical models. This knowledge of the model is replaced by a finite Element (FE) operator. In this paper, identification of complex Young's Modulus from measured displacement fields is shown using the FE model. To denoising the measured displacement a procedure based on a probabilistic approach coupled to a residue minimization is proposed. The method is illustrated on a curved beam using simulated displacement.

1 INTRODUCTION

The vibro-acoustic behavior of structures made of composite materials is difficult to grasp numerically, because the modeling of each constituent may lead to a huge model, which can not be operated. Such models can be reduced using for example homogenized material properties. However, obtaining these properties is not straightforward. The common methods to identify structural parameters can be divided in four categories. The first category corresponds to static or quasi-static methods, which are based on the linear elastic theory of materials [1]. Although these methods are well established, they provide incomplete information, in the sense that they do not allow to evaluate the frequency dependence of properties. The second category concern methods based on modal analysis [2]. They rely on the identification of natural frequencies and modal damping ratios to estimate the Young's Modulus and loss factor of a material. A third class of methods is based on

the finite element (FE) method. The principle is to model a structure and to compare the modal parameter numerically obtained (natural frequencies and mode shapes) with those measured on the real structure. The identification of structural parameters is performed by updating the FE model until the theoretical data match the experimental data [3]. The last family includes high frequency methods, also known as ultrasound methods [4], which may be used to obtain a spatial mapping of material properties.

At the end of 1990s, a new method was developed by Pézerat for vibration source identification [5] called Force Analysis Technique (FAT) or *Résolution Inverse Filtrée Fenêtrée* (RIFF), which stands for Windowed Filtered Inverse Resolution. This inverse method is based on the verification of the local equation of motion of a vibrating structure. As a consequence, the identification procedure can be performed locally on the structure and does not require the knowledge of the vibration field outside the area of interest. From the measurement of a local vibration field, this technique allows to obtain the distribution of external forces acting on the structure. To discretize the local equation of motion, the FAT method is based on a finite difference (FD) scheme. As the FD scheme amplifies the measurement noise, the inverse problem requires a regularization step. In the FAT method, the regularization is ensured by a spatial windowing associated with a low-pass filtering of the calculated force distribution. The main advantage of this method is that few informations are required: the local equation of motion and a local displacement field. Originally the method was developed only to identify sources on structures for which an analytical equation of motion exist, such as beams [6], plates [7] and shells [8].

To extend the FAT method and make it suitable for more complex structures, a Finite Element (FE) formulation of the inverse problem was developed by Renzi [9]. This variant of the method allows to identify nodal loads on a finite element mesh from the measured displacements. It has been experimentally validated on flexural beams and plates.

Another variant of the FAT method aims at identifying material properties (stiffness and damping). It is based on the verification of the local equation of motion in an area of the structure in which no external force applies. This method is independent of boundary condition and allows identification of material properties at any frequency, not only at resonances. The ability of the method to provide a spatial mapping of properties has been experimentally demonstrated by considering a composite plate containing patches of damping material [10]. Wassereau [11] extended this approach to characterize structural parameters on thick sandwich beams using Timoshenko's model. He estimated complex Young's Modulus and complex shear Modulus.

Recently, the two aforementioned variants of the FAT method have been coupled in an attempt to identify material properties on structure having complex geometries, using a FE operator. A proof-of-concept was presented considering a flat beam [12]. The estimation of a complex Young's Modulus was demonstrated using numerical and experimental data. The regularization of the inverse problem was introduced by a probabilistic approach inspired from previous work by Faure [13].

In this paper, this approach is extended to the case a curved beam, where coupling between flexural and membrane deformations occurs. In a first part, the general principle of the method is exposed. Then, the proposed approach is demonstrated using a simulated displacement field. Finally, the effect of noise is illustrated and a probabilistic framework is proposed to automatically adjust the level of regularization.

2 IDENTIFICATION TECHNIQUE

After previous development of the method on a straight beam [12], the considered case is now a curved beam. An essential difference between these two cases is the coupling occurring between traction motion and flexural motion. As a consequence, two Young's Moduli may be identified, one governing the axial stiffness E_t and the other one governing the bending stiffness E_f.

Let us consider the dynamic problem of an Euler-Bernoulli beam with length L_g, thickness h,

width b, section $S = h.b$ and second moment of area $I_z = b.h^3/12$. The materials properties are mass density ρ, axial complex Young's Modulus $\tilde{E_t} = E_t.(1 + j.\eta_t)$, where E_t is the axial Young's Modulus, η_t the axial structural loss factor and j the unit imaginary number, and flexural complex Young's Modulus $\tilde{E_f} = E_f.(1 + j.\eta_f)$, where E_f is the bending Young's Modulus, η_f, the bending structural loss factor.

Harmonic motion at angular frequency ω is considered. The beam is modeled by the Finite Element Method. The mesh consists of N nodes, corresponding to $N_{DOF} = 3N$ degrees of freedom (DOFs) and $N_e = N - 1$ elements. The dynamic matrix equation can be written as [14] :

$$\left(\mathbf{K} - \omega^2\mathbf{M}\right)\mathbf{u} = \mathbf{f}, \tag{1}$$

where $\mathbf{M}$ is the mass matrix, $\mathbf{K}$ is the dynamic stiffness matrix, $\mathbf{u}$ is the response vector consisting of nodal displacements and rotations and $\mathbf{f}$ is the vector of external forces and moments.

The matrices $\mathbf{M}$ and $\mathbf{K}$ are computed from the elementary matrices $\mathbf{M^e}$ and $\mathbf{K^e}$. The elementary matrices are basically expressed in the local coordinate system (x, y) of each beam element (see Fig. 1) as [14]:

$$\mathbf{M^e} = \rho S L_e \begin{bmatrix} \frac{1}{3} & 0 & 0 & \frac{1}{6} & 0 & 0 \\ 0 & \frac{13}{35} & \frac{11L_e}{210} & 0 & \frac{9}{70} & -\frac{13L_e}{420} \\ 0 & \frac{11L_e}{210} & \frac{L_e^2}{105} & 0 & \frac{13L_e}{420} & -\frac{L_e^2}{140} \\ \frac{1}{6} & 0 & 0 & \frac{1}{3} & 0 & 0 \\ 0 & \frac{9}{70} & \frac{13L_e}{420} & 0 & \frac{13}{35} & -\frac{11L_e}{210} \\ 0 & -\frac{13L_e}{420} & -\frac{L_e^2}{140} & 0 & -\frac{11L_e}{210} & \frac{L_e^2}{105} \end{bmatrix}, \tag{2}$$

and

$$\mathbf{K^e} = \begin{bmatrix} \frac{\tilde{E_t}S}{L_e} & 0 & 0 & -\frac{\tilde{E_t}S}{L_e} & 0 & 0 \\ 0 & \frac{12\tilde{E_f}I_z}{L_e^3} & \frac{6\tilde{E_f}I_z}{L_e^2} & 0 & -\frac{12\tilde{E_f}I_z}{L_e^3} & \frac{6\tilde{E_f}I_z}{L_e^2} \\ 0 & \frac{6\tilde{E_f}I_z}{L_e^2} & \frac{4\tilde{E_f}I_z}{L_e} & 0 & -\frac{6\tilde{E_f}I_z}{L_e^2} & \frac{2\tilde{E_f}I_z}{L_e} \\ -\frac{\tilde{E_t}S}{L_e} & 0 & 0 & \frac{\tilde{E_t}S}{L_e} & 0 & 0 \\ 0 & -\frac{12\tilde{E_f}I_z}{L_e^3} & -\frac{6\tilde{E_f}I_z}{L_e^2} & 0 & \frac{12\tilde{E_f}I_z}{L_e^3} & -\frac{6\tilde{E_f}I_z}{L_e^2} \\ 0 & \frac{6\tilde{E_f}I_z}{L_e^2} & \frac{2\tilde{E_f}I_z}{L_e} & 0 & -\frac{6\tilde{E_f}I_z}{L_e^2} & \frac{4\tilde{E_f}I_z}{L_e} \end{bmatrix}, \tag{3}$$

where L_e is the length of a beam element.

The stiffness elementary matrix (Eq. 3) can also be written as

$$\mathbf{K^e} = \tilde{E_t}\mathbf{K_t^e} + \tilde{E_f}\mathbf{K_f^e}, \tag{4}$$

where

$$\mathbf{K_t^e} = S \begin{bmatrix} \frac{1}{L_e} & 0 & 0 & -\frac{1}{L_e} & 0 & 0 \\ 0 & 0 & 0 & 0 & 0 & 0 \\ 0 & 0 & 0 & 0 & 0 & 0 \\ -\frac{1}{L_e} & 0 & 0 & \frac{1}{L_e} & 0 & 0 \\ 0 & 0 & 0 & 0 & 0 & 0 \\ 0 & 0 & 0 & 0 & 0 & 0 \end{bmatrix}, \tag{5}$$

is a matrix governing the axial stiffness of the element and

$$\mathbf{K_f^e} = I_z \begin{bmatrix} 0 & 0 & 0 & 0 & 0 & 0 \\ 0 & \frac{12}{L_e^3} & \frac{6}{L_e^2} & 0 & -\frac{12}{L_e^3} & \frac{6}{L_e^2} \\ 0 & \frac{6}{L_e^2} & \frac{4}{L_e} & 0 & -\frac{6}{L_e^2} & \frac{2}{L_e} \\ 0 & 0 & 0 & 0 & 0 & 0 \\ 0 & -\frac{12}{L_e^3} & -\frac{6}{L_e^2} & 0 & \frac{12}{L_e^3} & -\frac{6}{L_e^2} \\ 0 & \frac{6}{L_e^2} & \frac{2}{L_e} & 0 & -\frac{6}{L_e^2} & \frac{4}{L_e} \end{bmatrix}, \tag{6}$$

is a matrix governing the bending stiffness of the element.

Both matrices are formulated with respect to the local coordinate system (x, y). To obtain the assembled mass and stiffness matrices of Eq. (1), the elementary matrices have to be expressed in the global coordinate system (X_g, Y_g). For this purpose, a transformation matrix $\mathbf{T_e}$ is introduced [14], which allows to compute the mass and stiffness matrices of each element relative to the global coordinate system as

$$\mathbf{M_g^e} = \mathbf{T_e}^T \mathbf{M^e} \mathbf{T_e}, \tag{7}$$

and

$$\mathbf{K_g^e} = \mathbf{T_e}^T \mathbf{K^e} \mathbf{T_e} = \tilde{E}_t \mathbf{T_e}^T \mathbf{K_t^e} \mathbf{T_e} + \tilde{E}_f \mathbf{T_e}^T \mathbf{K_f^e} \mathbf{T_e}. \tag{8}$$

As seen, the separability property of the elementary stiffness matrix with respect to axial and bending behaviors is not altered by the coordinate transformation.

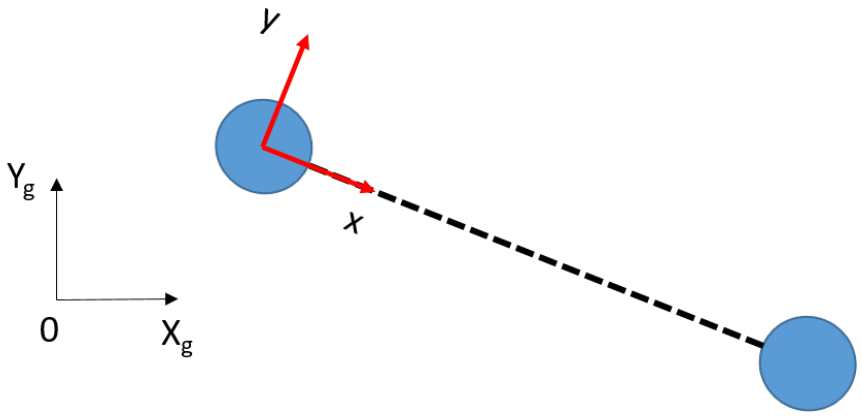

Figure 1: Two-dimensional beam element in arbitrary axes.

Then, the elementary matrices expressed in the global coordinate system are assembled to create the structural matrices $\mathbf{K}$ and $\mathbf{M}$ of Eq. (1). Since this process only involves matrix addition, it also does not alter the separability property expressed by Eq. (4) and propagated in Eq. (8).

Finally, considering a part of the beam where no external force or moment applies (i.e. where $\mathbf{f} = \mathbf{0}$), Eq. (1) can be rewritten as

$$\left(\tilde{E}_t \mathbf{K_t} + \tilde{E}_f \mathbf{K_f} - \omega^2 \mathbf{M}\right) \mathbf{u} = \mathbf{0}, \tag{9}$$

where $\mathbf{K_t}$ and $\mathbf{K_f}$ represent respectively the assembled matrices governing the axial and bending stiffness of the beam. This equation can be rewritten in a matrix form as

$$\left[\begin{array}{cc} \mathbf{K_t u} & \mathbf{K_f u} \end{array} \right] \left[\begin{array}{c} \tilde{E}_t \\ \tilde{E}_f \end{array} \right] = \omega^2 \mathbf{M u}. \tag{10}$$

Eq. (10) indicates that both Young's moduli $\tilde{E}_t$ and $\tilde{E}_f$ can be identified using a least square regression, if the nodal translations and rotations $\mathbf{u}$ are known.

3 NUMERICAL SIMULATIONS

3.1 Direct problem computed by FEM

In this section, a reference solution is calculated using the Finite Element Method (FEM). For this purpose, a clamped-clamped curved beam is considered (Fig. 2), whose characteristics are given in Table 1.

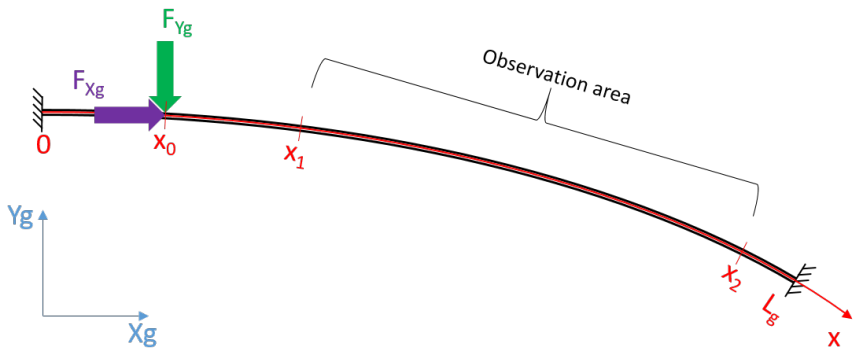

Figure 2: Geometry of beam used for numerical simulation.

Length L_g (m)	Width b (m)	Thickness h (m)
1	0.01	0.001
Second moment of area I (m^4)	Density ρ (kg/m^3)	Axial Young's Modulus E_t (GPa)
$b \cdot h^3/12$	2700	75
Traction loss factor η_t	Bending loss factor η_f	Bending Young's Modulus E_f (GPa)
0.1 %	0.1 %	70
Spatial sampling L_e (m)	Frequency (Hz)	Amplitude of excitation $\lvert F_{X_g} \rvert$ and $\lvert F_{Y_g} \rvert$ (N)
0.01	5000	1
Excitation location x_0 (m)	Observation area $[x_1; x_2]$ (m) in curvilinear abscissa	
0.1	[0.3 ; 0.8]	

Table 1: Geometrical and materials properties set for the simulated beam and excitation characteristics.

The displacement field $\mathbf{u}$ (translations and rotations) is computed at discrete abscissas delimited by $x \in [0.3; 0.8]$ m, i.e. in a region not directly excited by external forces of moments (see Fig. 3). The displacement field is then blurred with noise,

$$\mathbf{u}_{noisy} = \mathbf{u} + 10^{\frac{-SNR}{20}} \boldsymbol{\alpha}, \tag{11}$$

where $\mathbf{u}_{noisy}$ denotes the noisy displacements, α is a zero mean Gaussian random variable with unit variance and the Signal to Noise Ratio (SNR) is set at 40 dB.

3.2 Numerical inverse problem

The aim of the inverse problem is to identify Young's moduli E_f and E_t from the measured displacement field. First, the feasibility of the proposed method with exact data is shown. Then, the problem arising from noisy measurements will be illustrated. In the next section, a regularization procedure allowing the identification of Young's moduli will be proposed.

As stated above, the inverse problem is based on verifying the equilibrium between stiffness and inertia terms of Eq. (1) in an area where no external effort applies, i.e. where Eq.(9) is expected to be verified. A first issue related to the practical use of Eq. (9) on a subdomain of the beam concerns the existence of efforts at the boundaries of the observation area (Figure 4). These efforts correspond to forces and moments exerted by the adjacent parts of the beam on both sides. As a result, the left hand side of Eq. (9) is actually zero valued everywhere except at boundaries, as shown in Figure 4.

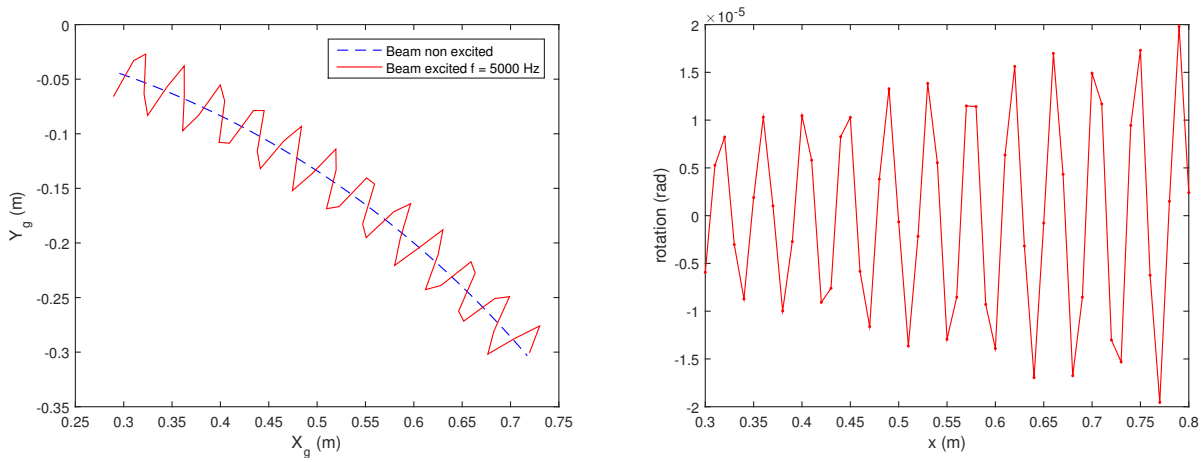

(a) (b)

Figure 3: Displacements in observed area: (a) Translations (scale $\times 1000$) in the global axes, (b) Rotation displacement along the curvilinear abscissa of the beam.

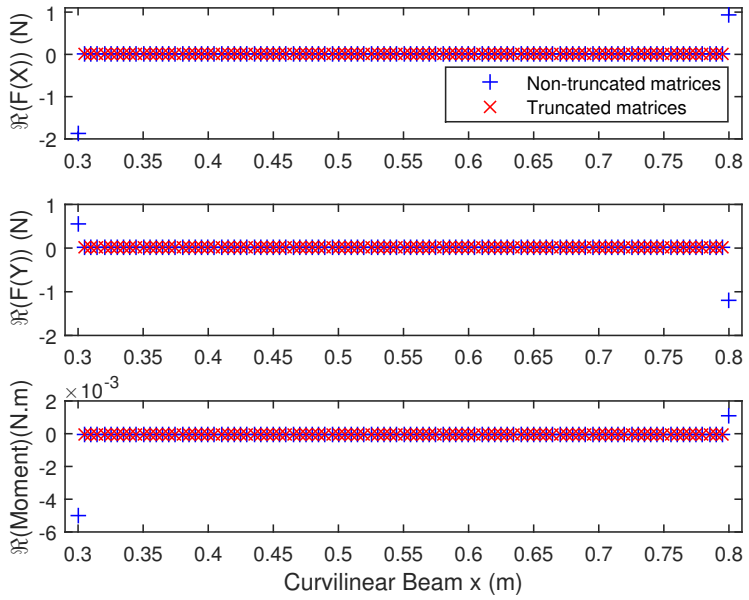

Figure 4: External efforts in the beam calculated from the left hand side of Eq. (9), using non-truncated or truncated stiffness and mass matrices.

A way to avoid these efforts is to truncate mass and stiffness matrices, by removing the first three and last three lines. This corresponds to ignoring the three external efforts (2 forces and 1 moment) at each end, which ensures that Eq. (9) is fully verified (see Fig. 4). In the following, the truncated matrices are simply denoted by $\mathbf{K_t}$, $\mathbf{K_f}$ and $\mathbf{M}$ to keep a good readability.

3.3 Principle of regularization

In this section, a probabilistic framework is introduced to regularize the inverse problem when noisy data is considered.

Taking into account explicitly the noise perturbation coming from the measurement, the observation equation can be written as

$$\mathbf{u}_{noisy} = \mathbf{u} + \mathbf{n}, \tag{12}$$

where $\mathbf{n}$ denotes the vector of noise. Considering white noise, the probability of $\mathbf{n}$ can be written as

$$\mathbf{n} \sim \mathcal{N}_c(\mathbf{0}, \sigma_n^2 \cdot \mathbf{I}), \tag{13}$$

which represents a multivariate complex Gaussian distribution with zero mean and variance σ_n^2. Substituting Eq. (13) into the observation equation Eq. (12) provides the probability of exact displacements

$$\mathbf{u} \sim \mathcal{N}_c(\mathbf{u}_{noisy}, \sigma_n^2 \cdot \mathbf{I}), \tag{14}$$

It has been observed that the calculation of $\mathbf{K_t u}_{noisy}$ and $\mathbf{K_t u}_{noisy}$ is responsible for the instability of the inverse problem, since it drastically amplifies measurement noise (for the sake of brevity these results are not shown in the paper). For this reason, the proposed regularization procedure consists in estimating the term

$$\boldsymbol{\delta} = \tilde{E}_t \mathbf{K_t u} + \tilde{E}_f \mathbf{K_f u}. \tag{15}$$

This can be done by merging the probabilistic information provided by two equations. A first equation corresponds to the direct estimation of $\boldsymbol{\delta}$ from noisy displacements using Eq. (15). Substituting Eq. (14) into Eq. (15) provides the probability

$$\boldsymbol{\delta} \sim \mathcal{N}_c(\tilde{E}_t \mathbf{K_t u}_{noisy} + \tilde{E}_f \mathbf{K_f u}_{noisy}, (\tilde{E}_t \mathbf{K_t} + \tilde{E}_f \mathbf{K_f}) \sigma_n^2 (\tilde{E}_t \mathbf{K_t} + \tilde{E}_f \mathbf{K_f})^H), \tag{16}$$

where superscript H denotes the Hermitian transpose. A second equation is related to the a priori verification of the equation of motion Eq. (9), i.e.

$$\boldsymbol{\delta} = \omega^2 \mathbf{M u}. \tag{17}$$

Substituting Eq. (14) into Eq. (17) provides the probability

$$\boldsymbol{\delta} \sim \mathcal{N}_c(\omega^2 \mathbf{M u}_{noisy}, (\omega^2 \mathbf{M}) \sigma_n^2 (\omega^2 \mathbf{M})^H). \tag{18}$$

A regularized estimate of $\boldsymbol{\delta}$ can therefore be obtained from the intersection of both probabilities, i.e. the product of the two Gaussian distributions of Eqs. (16) and (18),

$$[\boldsymbol{\delta}] \propto \mathcal{N}_c(\boldsymbol{\mu}_{\boldsymbol{\delta_1}}, \boldsymbol{\Sigma}_{\boldsymbol{\delta_1}}) \cdot \mathcal{N}_c(\boldsymbol{\mu}_{\boldsymbol{\delta_2}}, \boldsymbol{\Sigma}_{\boldsymbol{\delta_2}}), \tag{19}$$

where

$$\begin{cases} \boldsymbol{\mu}_{\boldsymbol{\delta_1}} = \tilde{E}_t \mathbf{K_t u}_{noisy} + \tilde{E}_f \mathbf{K_f u}_{noisy} \\ \boldsymbol{\Sigma}_{\boldsymbol{\delta_1}} = (\tilde{E}_t \mathbf{K_t} + \tilde{E}_f \mathbf{K_f}) \sigma_n^2 (\tilde{E}_t \mathbf{K_t} + \tilde{E}_f \mathbf{K_f})^H \\ \boldsymbol{\mu}_{\boldsymbol{\delta_2}} = \omega^2 \mathbf{M u}_{noisy} \\ \boldsymbol{\Sigma}_{\boldsymbol{\delta_2}} = (\omega^2 \mathbf{M}) \sigma_n^2 (\omega^2 \mathbf{M})^H. \end{cases} \tag{20}$$

The result is itself a Gaussian distribution,

$$[\boldsymbol{\delta}] \propto \mathcal{N}_c(\boldsymbol{\delta} | \boldsymbol{\mu}_{\boldsymbol{\delta}}, \boldsymbol{\Sigma}_{\boldsymbol{\delta}}), \tag{21}$$

where the mean vector and covariance matrix are given by

$$\begin{cases} \boldsymbol{\Sigma}_{\boldsymbol{\delta}} = \left({\boldsymbol{\Sigma}_{\boldsymbol{\delta_1}}}^{-1} + {\boldsymbol{\Sigma}_{\boldsymbol{\delta_2}}}^{-1} \right)^{-1} \\ \boldsymbol{\mu}_{\boldsymbol{\delta}} = \boldsymbol{\Sigma}_{\boldsymbol{\delta}} \left({\boldsymbol{\Sigma}_{\boldsymbol{\delta_1}}}^{-1} \boldsymbol{\mu}_{\boldsymbol{\delta_1}} + {\boldsymbol{\Sigma}_{\boldsymbol{\delta_2}}}^{-1} \boldsymbol{\mu}_{\boldsymbol{\delta_2}} \right) \end{cases} \tag{22}$$

In the following, the MAP (Maximum A Posteriori) estimate of $\boldsymbol{\delta}$, i.e. $\boldsymbol{\mu}_{\boldsymbol{\delta}}$, is considered. It can be shown from Eqs (20) and (22) that $\boldsymbol{\mu}_{\boldsymbol{\delta}}$ finally does not depend on σ_n. As a consequence, no a priori knowledge of noise level is required to perform the regularization.

3.4 Regularized results on noisy data

In the previous section, a regularized estimate of the left hand side of Eq. (10) has been derived. In contrast, it has been shown in a previous paper [12] that the term $\mathbf{M}\mathbf{u}_{noisy}$ does not notably amplifies the measurement noise. For this reason, no regularized expression is seeked for this term.

Following this and Eq. (10), the result of $\boldsymbol{\mu_\delta} - \omega^2\mathbf{M}\mathbf{u}_{noisy}$ should be close to zero when the Young's moduli $\tilde{E}_t$ and $\tilde{E}_f$ are close to their actual values. To perform the identification of these moduli, a cost function

$$f(\tilde{E}_t, \tilde{E}_f) = \sum |\boldsymbol{\mu_\delta} - \omega^2\mathbf{M}\mathbf{u}_{noisy}|^2. \tag{23}$$

is introduced, where the dependence on $\tilde{E}_t$ and $\tilde{E}_f$ is carried by $\boldsymbol{\mu_\delta}$ (see Eqs (20) and (22)). The result of this cost function should be interpreted as an indication of the residual efforts in the right hand side of Eq. (9).

Figure 5 (a) shows the residue for different values of Young's Modules. Here, the displacement $\mathbf{u}$ is exact. A minimum residue is clearly obtained and points to the correct values of Young's Modules. Young's Modules can also be identified.

When noise is added to displacement, Figure 5 (a) becomes Figure 5 (b). It can be observed that Young's Modules are unidentified.

After regularisation and optimisation, on Figure 5 (c), it seems that E_f is correctly identified but E_t not. If a research of minimum is done, the traction Young's Modulus is also well identified.

This new developed method with this regularisation is applied on a large band of frequencies, between $100\ Hz$ and $10000\ Hz$. Figure 6 (a) and (b) show the result of the parameters identification.

It can be observed that the bending Young's Modulus is correctly identified at any frequencies. However some difficulties arise at some singular frequencies where the structure is excited on nodal point. For the traction/compression Young's Modulus, the identification seems to be more complicated, especially in the low frequency domain. Concerning loss factor, Figure 6 (b) shows the difficulty to obtain accurate results.

4 CONCLUSION

Continuing the work for the identification of materials properties on a straight beam, this paper presented the extension of the same method for a curved beam where the identification of Young's Modulus in traction/compression and in bending is proposed. The developed method is based on the RIFF method coupled to a Finite Element operator. The use of this method is conditioned by the knowledge of the structure geometry, to build stiffness and mass matrices, by the assurance no force is applied on the observation area and the access of the displacement field. To overcome to the noise issue, a probabilistic approach coupled to a residue minimization is used.

This method has been validated on a simulated beam for a wide frequency band. It allows also to identify material properties, like complex Young's Modules in traction/compression and in bending.

Finally, the effect of the curvatures on both equivalent Young's modules will be studied in order to propose more simple FEM operator to model structures in composite materials.

ACKNOWLEDGEMENTS

This study is part of the RICTUS project managed by IRT Jules Verne (French Institute in Research and Technology in Advanced Manufacturing Technologies for Composite, Metallic and Hybrid Structures).

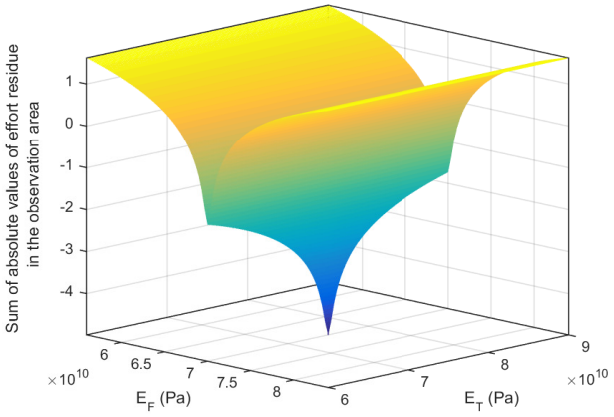

(a)

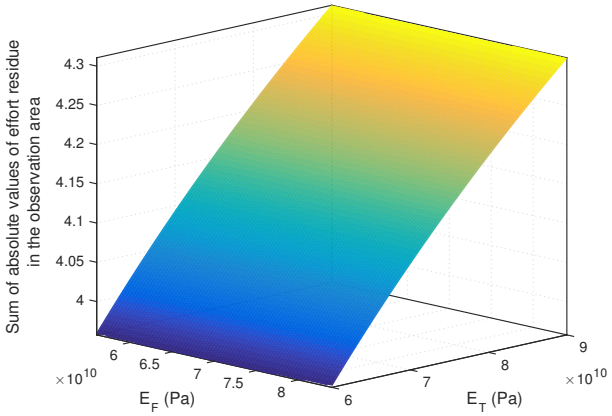

(b)

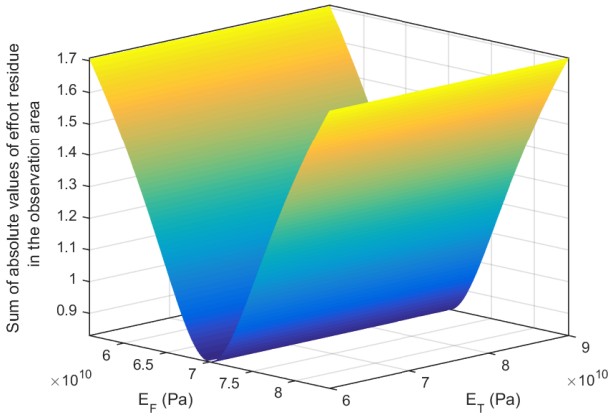

(c)

Figure 5: Surface of effort residue in function of traction and bending Young's Modules: (a) Exact data, (b) Noisy data non regularized and (c) Noisy data regularized.

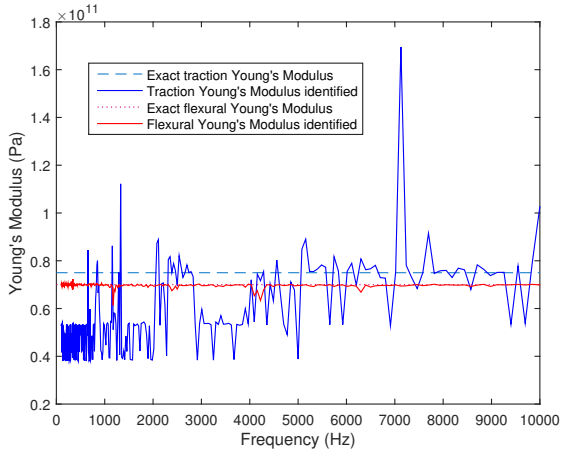

(a)

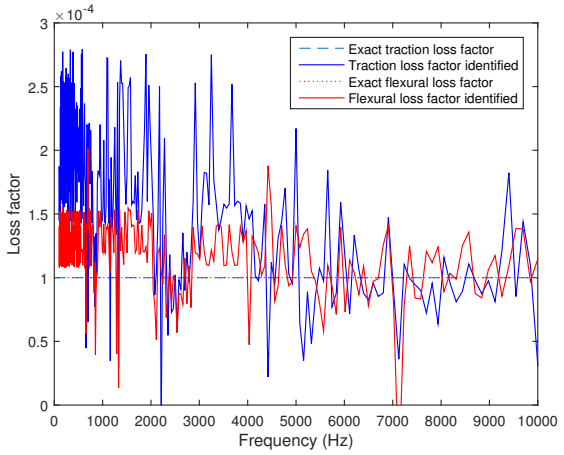

(b)

Figure 6: Identification of complex Young's Modules for a large frequency band: (a) Young's Modules in traction/compression and in bending and (b) Loss factors in traction/compression and in bending.

REFERENCES

[1] K. P. Menard. *Dynamic Mechanical Analysis: A Practical Introduction*. CRC Press, 2nd edition, 2008.

[2] D. J. Ewins. *Modal Testing: Theory, Practice and Application*. Research Studies Press, 2nd edition, 2000.

[3] P. Blaschke and T. Schneider. *Reactionless Test to Identify Dynamic Young's Modulus and Damping of Isotropic Plastic Materials*, pages 511–516. Springer New York, New York, NY, 2014.

[4] C. Potel, T. Chotard, J-F. de Belleval, and M. Benzeggagh. Characterization of composite materials by ultrasonic methods: modelization and application to impact damage. *Composites Part B: Engineering*, 29(2):159 – 169, 1998. High Temperature Composites and Interfaces: Analysis, Processing and Characterization.

[5] C. Pezerat. *Method of identification of forces applied on a vibrating structure, by resolution and regularization of the inverse problem*. Theses, INSA de Lyon, December 1996.

[6] C. Pézerat and J.-L. Guyader. Two inverse methods for localization of external sources exciting a beam. In *Acta Acustica*, volume 3, pages 1–10, 1995.

[7] C. Pézerat and J.L. Guyader. Force analysis technique: reconstruction of force distribution on plates. *Acta Acust.*, 86(2):322–332, 2000.

[8] M.C. Djamaa, N. Ouelaa, C. Pezerat, and J.L. Guyader. Reconstruction of a distributed force applied on a thin cylindrical shell by an inverse method and spatial filtering. *Journal of Sound and Vibration*, 301(3):560 – 575, 2007.

[9] C. Renzi. *Identification expérimentale de sources vibratoires par résolution du probléme inverse modélisé par un opérateur éléments finis local*. Theses, INSA de Lyon, December 2011.

[10] F. Ablitzer, C. Pézerat, J-M. Génevaux, and J. Bégué. Identification of stiffness and damping properties of plates by using the local equation of motion. *Journal of Sound and Vibration*, 333(9):2454 – 2468, 2014.

[11] T. Wassereau. *Caractérisation de matériaux composites par problème inverse vibratoire*. phdthesis, Université du Maine, October 2016.

[12] P. Bottois, N. Joly, C. Pézerat, and F. Ablitzer. Identification of local young's modulus and loss factor of curved beam by using an inverse method and a finite element operator. *INTER-NOISE and NOISE-CON Congress and Conference Proceedings*, 255(5):2165–2174, 2017.

[13] C. Faure. *Approches bayésiennes appliqués à l'identification d'efforts vibratoire par la méthode de Résolution Inverse*. PhD thesis, Le Mans Université, 2017.

[14] M. Géradin and D. Rixen. *Théorie des vibrations, Application à la dynamique des structures*. MASSON, 2è edition, 1996.